Novel Pumping System based on Micro-Hydro Turbine and Centrifugal Pump coupled using EVT Induction Machine. Application in Rural Area Irrigation.

MARCELO G. CENDOYA, SANTIAGO A. VERNE, PEDRO E. BATTAIOTTO
Instituto de Investigaciones en Electrónica, Control y Procesamiento de Señales (LEICI)
UNLP - CONICET - CIC PBA
Departamento de Electrotecnia, Facultad de Ingeniería
Universidad Nacional de La Plata
Calle 1 y 47, La Plata (B1900TAG, Buenos Aires
ARGENTINA

Abstract: - In this article, a topology for energy conversion oriented to water pumping for irrigation in remote areas is proposed. A micro-hydraulic turbine working at fixed speed, in a "run-off-river" configuration, drives a centrifugal pump through a variable electric transmission (EVT). An EVT based on induction machines was selected, with the stator directly connected to a weak AC grid but the internal rotor fed by a variable frequency drive, allowing an adjustable pump speed. The grid supplies a base power for residential consumption, while the hydro turbine increases the available power for irrigation and thus augmenting productivity of the land uphill and beyond the vicinity of the watercourse. The grid also provides an assistance function, absorbing/delivering a reduced amount of power in case the hydraulic resource is excessive/insufficient for the requested water pumping.
As the turbine delivery is constant, the water pumping requirement establishes the power exchanged between turbine, AC grid and pump. For this reason, an analysis to quantify the power flow in the system components for different pump speeds has been carried out. The system modeling is described and computer simulations, using a specific pump speed profile, are presented to validate the performed theoretical analysis.

Key-Words: - Electric Variable Transmission; Micro-hydro Turbines; Water Pumping; Weak Grids.

Received: September 23, 2022. Revised: February 19, 2023. Accepted: March 18, 2023. Published: May 8, 2023.

1 Introduction

The availability of water and renewable energy in rural areas far from cities is vital for the economic and productive development of a region. Fortunately, Argentina has many water resources, especially in the adjacent area near to Los Andes Mountains and in the northern region. Additionally, the territory is suitable for growing various species such as grapevines, olives, and fruits, which are the stronger productive industries in that region [1] [2]. Moreover, these crops increase their productivity by optimizing the irrigation regime, especially considering the scarce rainfall and low humidity levels. For this reason, the exploitable territory is close to watercourses. However, the traditional runoff irrigation method presents a low efficiency of water usage, about 65%, and it is highly restricted by the characteristic land conditions. In this sense, drip or micro-sprinkler irrigation is a promising technology to increase both water usage in rational form and land productivity, since it allows for the exploitation of lands in higher elevations with uneven surfaces, and relatively far from water resources [3]-[6].

The infrastructure of such an irrigation system consists of a pressurized water distribution network through pipes, pumping systems, and a power supply. Frequently, productive areas are not reached by the electrical utility grid, and a significant part of the energy requirements are supplied by diesel fuel. However, due to the constant decrease in costs, renewable energies tend to provide viable solutions [7] [8]. Sometimes, a weak grid reaches the site, but its power capacity is limited in quantity and/or quality. However, areas that have surface water resources, such as waterfalls or small streams, can be used to convert the energy of water into another type of energy, typically electricity. In the power range of less than 100 kW, such facilities are called micro-hydropower plants and constitute a very attractive energy conversion technology that allows for the supply of reliable and constant energy in an isolated form or interconnected to a grid [9] [10].

Many primary energy sources come in the form of mechanical power. Then, equipment usually converts it into electricity which is easily distributed among loads. In water pumping systems, the electrical energy from the renewable sources is used to power the variable speed pumps through electric motors fed by variable frequency drives (VFD's) [11] [12]. However, this topology involves a double conversion (mechanical-electrical-mechanical) of the entire power which lowers the overall efficiency, due to losses in each conversion stage. A variable electrical transmission (EVT) is an electromagnetic conversion device based on an electric machine with two mechanically decoupled shafts and two electric ports [13]. EVT integrates a driving machine and a load machine into a single machine that allows the conversion of mechanical energy between both shafts. On the other hand, although electronic converters are required to control the power flow, it is possible to undersize them to a fraction of the power in EVT`s mechanical ports [14]. Therefore, an EVT is a promising device for mechanical conversion applications such as electric vehicle propulsion and even as a gearbox in wind turbines [15][16].

This paper proposes a hydraulic energy conversion system, connected to a weak grid, that is oriented to irrigation purposes. The local generation source is based on a propeller type (also known as semi-Kaplan due to the fixed pitch angle) micro-hydraulic turbine, whose main function is to provide a power increase (above the power level available from the weak grid) needed to augment the capacity of the water pumping system. The turbine is linked to a centrifugal pump through an EVT. As the stator of the EVT input shaft is connected to the grid, the turbine operates at fixed speed. On the other hand, the internal rotor of the EVT is fed by a VFD, allowing an adjustable output shaft speed, where there is the centrifugal pump.

Section 2 describes the architecture of the irrigation system under study and presents the mathematical model of each component. In Section 3 is carried out an analysis of the power distribution in different working conditions, which are determined by the pumping requirements. Section 4 shows computer simulations made to validate the foregoing analysis, accompanied by a discussion of the obtained results. Finally, the conclusions of the work done are outlined.

2 System Description

Figure 1 shows the geographical scenario for the irrigation system. At a certain height, part of the flow is diverted from the main channel of the watercourse. The civil works for the diversion channel could be carried out ad-hoc or even be previously existing [9][17][18]. In both cases, the micro-hydro power plant is located inside the powerhouse, at the bottom of the channel. The water intake may include a natural or built reservoir in the upper part of the turbine feeding pipe (penstock). Subsequently, a desanding/load chamber removes particles which could damage the turbine and eliminates possible turbulences prior to the discharge through the penstock. The outlet of the penstock supplies the water flow for the turbine, which is attached to the EVT input shaft, whilst the turbine discharge returns to the watercourse. The centrifugal pump is linked to the EVT output shaft, and its outlet supplies the necessary filling flow (through the main pipe) to maintain an adequate level in the irrigation water reservoir, which is located at a higher height than the powerhouse. To not disturb the water flowing through the turbine, the inlet of the centrifugal pump is fed from the turbine discharge. This is possible since the pump must supply a relatively low flow to a water reservoir located at a considerable height, contrary to the turbine that operates at a low head and a higher flow (remember that the hydraulic power depends on the product of the head times the flow; furthermore, the hydraulic power of the turbine and the pump are comparable in this case).

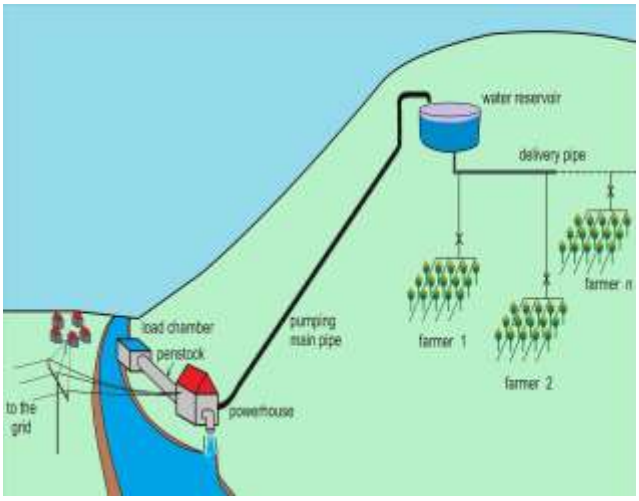

Fig.1: Geographical distribution of the irrigation system.

Figure 2 shows the mechanical coupling between the turbine and the pump through the EVT, and its electrical connections. A weak AC distribution grid is supplying the residential loads. A link (ACN) connects the EVT to the weak grid. As mentioned in the Introduction, the micro turbine is coupled to the input shaft of the EVT (external rotor), whose stator is directly connected to ACN without any electronic conversion, which is possible because this part of the EVT behaves like a conventional squirrel cage induction generator (a more detailed description of the EVT will be given in the following section). This causes the turbine speed to remain in a small interval around the synchronous speed, which is set by the weak grid electrical frequency. In this typical situation (ignoring the small speed slip), the turbine is said to be operating at "fixed speed". The centrifugal pump is coupled to the output shaft of the EVT (internal rotor), whose winding is fed by a VFD, also connected to ACN. The use of a VFD allows adjusting the speed of the centrifugal pump in an ample range. The speed reference signal for the VFD is generated from an external control loop that regulates the water level in the irrigation water reservoir at some desired value.

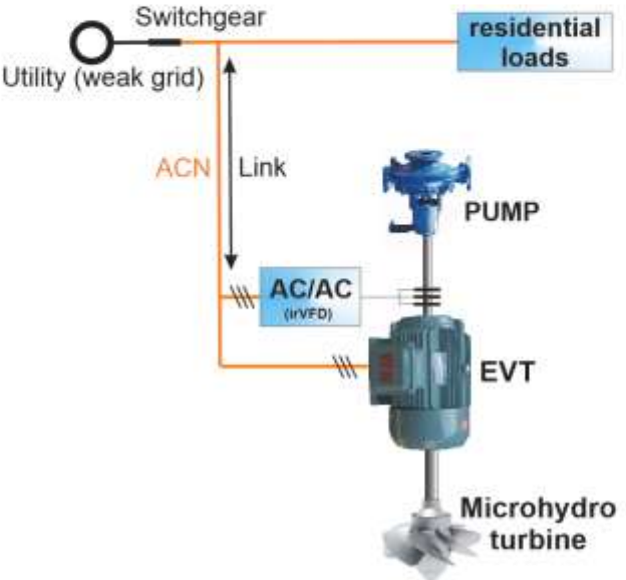

Fig.2: Turbine and pump mechanical coupling and EVT electrical connections.

2.1 Micro Hydro Turbine

In this work it is considered the use of a semi-Kaplan micro-hydro turbine, also known as a "propeller" turbine because (unlike the standard Kaplan turbine) the blades have a fixed pitch angle. This is an axial flow turbine that, due to its design features, is well-suited for low to moderate heads (less than 40m), where water flow is relatively high [19]. The turbine is located inside the powerhouse at a low level of the terrain, to establish a sufficient head. The hydraulic power P_H of a water flow Q falling from a net head H (which is the actual static head minus the dynamic head that represents the friction losses in the penstock) can be calculated as:

$$P_H = \rho g H Q \tag{1}$$

In (1) ρ is the water density (1000 kg/m^3) and g is the acceleration due to gravity (9.8m/s^2). A hydraulic turbine converts only a fraction of the total hydraulic power P_H into mechanical power P_T on its shaft, that is the product of the turbine mechanical torque T_T and the shaft rotating speed ω_T. This fraction is called the turbine conversion efficiency η_T:

$$P_T = T_T \omega_T = \eta_T P_H \tag{2}$$

The mechanical power and the turbine efficiency are variable depending on H, Q, and ω_T. There is an optimal operating point in which the mechanical power reaches its maximum value [20]. The optimal operating speed ω_{Topt} of a semi-Kaplan turbine, for a given values of H and Q, can be determined using the following formula [21]:

$$\omega_{Topt} = \sigma (2gH)^{\frac{3}{4}} / 2\sqrt{\pi Q} \tag{3}$$

In (3), σ is a characteristic design parameter that depends on H and whose typical value can be found in [21].
To make approximate evaluations by computer simulation in a preliminary project stage (for example, to design and tuning a controller), it is possible to use a simplified mathematical expression for the torque developed by the turbine, such as the one that can be found in [22]:

$$T_T = T_o (1 - \omega_T / \omega_{Tmax}) \tag{4}$$

In (4) T_o is the turbine starting torque (when ω_T=0) and ω_{Tmax} is the turbine runaway rotating speed (when T_T=0). The expression (4) is valid only when the turbine operates with a constant head and a constant flow rate. In our case, as the penstock is usually fed from the discharge of a small reservoir that has a relief duct, (which means that it stays completely full most of the time), the head will be constant. On the other hand, as the flow depends on the head and the rotating speed of the turbine (both constant quantities in our case), one can conclude that the flow will also be a constant magnitude. Therefore, the use of (4) is completely justified for the situation under analysis. If (4) is assumed to be valid, then the mechanical power delivered by the turbine at is shaft is:

$$P_T = T_o(\omega_T - \omega_T{}^2/\omega_{Tmax}) \quad (5)$$

From (5) the maximum power of the turbine can be derived:

$$P_{Tmax} = T_o\omega_{Tmax}/4 \quad (6)$$

which occurs at an optimal rotational speed ω_{opt}:

$$\omega_{opt} = \omega_{Tmax}/2 \quad (7)$$

Equations (4) and (5) are depicted in Figure 3, which shows the maximum mechanical power point, defined by (6), and a selected operating point (A) (P_{TA}, n_{TA}) slightly shifted to the left as in [22].

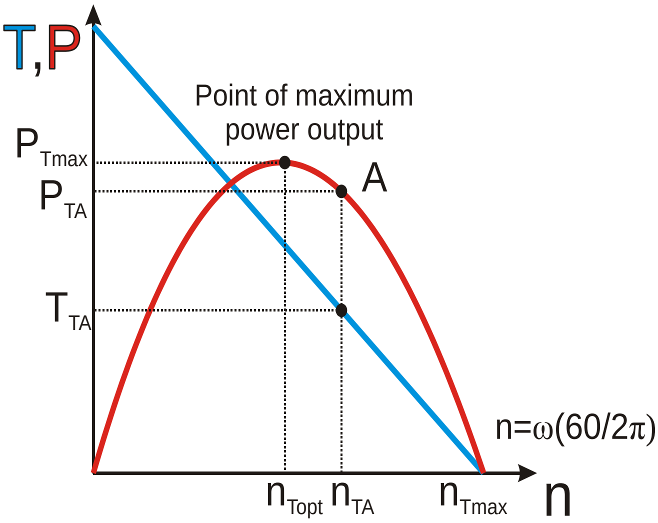

Fig.3: Torque/Power - speed characteristic of the turbine.

2.2 Electric Variable Transmission (EVT)

As already mentioned, to couple the fixed speed micro-hydro turbine to the variable speed centrifugal pump, an EVT machine is employed. Figure 4 shows the simplified physical structure of the EVT. The electrical and electromechanical power flows are denoted with arrows which describe their possible directions, depending on the working conditions of each EVT shaft. A three-phase stator winding is located on the yoke of the EVT, that is identical to a standard induction machine and, in our application, is directly connected to the grid. It produces a rotating magnetic field whose speed (known as "synchronous speed") is established by the grid frequency. Internal to the yoke there is a cup-shaped rotor (hereinafter called interrotor).

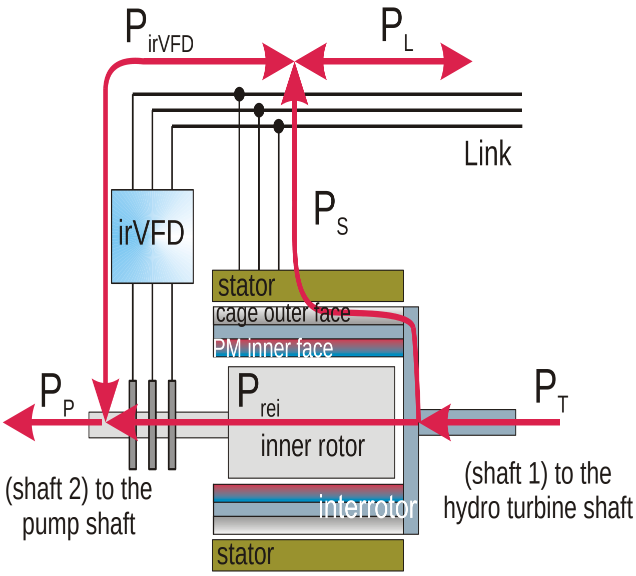

Fig. 4:. EVT machine physical diagram and power flow.

There are some constructive variants for the interrotor of an EVT: both faces with permanent magnets (PM), both faces with squirrel cage, wounded interrotor, etc. [13] [23]. In this work, an EVT with a hybrid interrotor, like the one presented in [23], is used. In this type of EVT, the outer face of the interrotor has short-circuited conductive bars, forming a squirrel cage. This allows direct connection to the grid in a simple way. If PMs would be used in the outer face of the interrotor, some kind of synchronization with the grid frequency would be required. The outer face interrotor squirrel cage interacts with the rotating magnetic field produced by the stator and defines an "EVT External Induction Machine". Otherwise, PMs located at the interrotor inner face produce a magnetic field that rotates at the interrotor mechanical speed. Internally to the interrotor, there is the inner rotor, that has a three-phase winding (similar way to a DFIM machine) with slip rings fed from a variable frequency drive (irVFD) to set currents with the desired amplitude and frequency. The inner rotor winding interacts with the rotating magnetic field produced by the PMs, defining an "EVT Internal Induction Machine".

It has been decided to use the stator winding of the EVT External IM directly connected to the grid, because in this way the use of an expensive converter is avoided, also obtaining greater simplicity and reliability. In this manner, simple and cheap soft starter equipment is required for the connection to the grid.

As the interrotor is mechanically joined to the turbine, the rotating speed variation is determined by:

$$d\omega_T/dt = (T_T - T_{EM1} - T_{EM2})/J_T \quad (8)$$

In (8), J_T is the total moment of inertia considering all the rotating masses linked to the input shaft, T_T is the torque provided by the hydro turbine, given by (4), T_{EM1} is the electromagnetic torque that arises from the interaction of the magnetic rotating field of the stator and the magnetic field produced by the bars of the outer face of the interrotor. T_{EM2} is the electromagnetic torque that arises from the interaction between magnetic field provided by PMs located at the inner face of the interrotor and the magnetic field produced by the winding of the inner rotor (which is mechanically transmitted through the mechanical structure of the interrotor to the input shaft).

The magnetic field produced by the EVT External IM stator, rotates at the synchronous speed ω_S given by:

$$\omega_S = 2\pi f_{e1}/p_1 \quad (9)$$

where f_{e1} is the grid frequency and p_1 is the number of pole pairs of the stator winding. As in any conventional induction machine, for torque production it is necessary that the interrotor rotates at a slightly different speed than ω_S. At normal working conditions the interrotor speed is close to the synchronous speed. In this situation, called “low slip operation”, it is possible to calculate T_{EM1} using a linear approximation given by [24]:

$$T_{EM1} = K_G(\omega_T - \omega_S) \quad (10)$$

where K_G is the slope of the torque-speed characteristic. This value depends on the magnetic flux amplitude in the air gap between the stator and the interrotor and the resistance of the interrotor outer face bars.

As the inner rotor is mechanically coupled to the centrifugal pump, the variation of the EVT output shaft speed ω_P is described by the following expression:

$$d\omega_P/dt = (T_{EM2} - T_P)/J_P \quad (11)$$

In (11), J_P is the total moment of inertia considering all rotating masses linked to the EVT output shaft and T_P is the resistant torque presented by the centrifugal pump. This torque can be calculated as [25]:

$$T_P = K_P{\omega_P}^2 \quad (12)$$

where K_P is a constant, specific for each pump model, that depends on its design characteristics [25].

It can be noticed from (11) that T_{EM2} determines the operating speed of the pump but also affects the EVT input shaft speed, as seen in (8). Usually, the time constants of both the VFD and the inner rotor winding are much faster than those of the mechanical and hydraulic parts of the system. For this reason, it is possible to use the steady state value of T_{EM2} to evaluate (11). In steady state and low slip operation, the value of T_{EM2} follows an approximately linear fashion with respect to the difference in rotational speeds between the interrotor, and the inner rotor:

$$T_{EM2} = K_M(\omega_T + \omega_C - \omega_P) \quad (13)$$

In (13), K_M is the slope of the torque-speed characteristic, and its value depends on the flux amplitude in the air gap between the interrotor and the inner rotor (produced by the PMs) and the inner rotor winding resistance. It should be noticed that ω_T acts as the synchronous speed for the inner rotor, as it is the speed of the rotating PMs. On the other hand, ω_C represents the abscissa displacement suffered by the torque-speed characteristic, that depends on the frequency value f_{e2} provided to the inner rotor winding by the VFD:

$$\omega_C = 2\pi f_{e2}/p_2 \quad (14)$$

In (14), p_2 is the pole pairs number of the inner rotor.

2.3 Water Reservoir

The variation of the water level h_r in a reservoir with vertical walls is described by:

$$dh_r/dt = (Q_P - Q_C)/A_r \quad (15)$$

A_r is the reservoir base area, Q_P is the water flow rate supplied by the centrifugal pump and Q_C is the water flow rate consumed by the irrigation system.

Considering the well-known “affinity laws” [26], it can be assumed that the water flow rate supplied by the pump is related to its rotational speed as:

$$Q_P = K_Q\omega_P \quad (16)$$

In (16), K_Q is a constant that depends on the pump design characteristics and the associated hydraulic circuit.

3 System Power Distribution Analysis

As stated earlier, the grid frequency forces the turbine to work at almost fixed speed. This situation, together with the fact that the head does not change, makes the water flow through the turbine remain constant as well. Considering the principle of operation of the turbine, that was explained in subsection 2.1, it is easy to see that the mechanical power delivered by the turbine to the input shaft of the EVT has a near constant value. On the other hand, the centrifugal pump speed needs to be regulated to supply the changing flow of water required for irrigation. This changing speed causes the mechanical power taken by the pump from the EVT output shaft to be also variable. It may then happen that the power required by the pump is less than that supplied by the turbine or, conversely, that it is greater than it. This power imbalance means that the difference must be absorbed or supplied by the weak grid. To do this, there are two possible paths: through the EVT stator winding or through the VFD (it can manage power in a bidirectional way) and which is also linked to the weak grid. At this point, the need for a detailed analysis of how the power is exchanged between all the elements of the system arises.

First, to carry out the analysis we must establish certain starting hypotheses and considerations:

1) A turbine with a rated mechanical output power of P_T=50kW for the speed of n_T=1000RPM, was selected.

2) An EVT stator winding with three pole-pairs was used. According to (9), for p_1=3 and considering a 50Hz grid frequency, the resulting synchronous speed of the External Induction Machine is n_S=1000RPM (as given in (9) multiplied by $60/2\pi$).

3) A three pole-pairs of permanent magnets arrangement (fixed to the inner face of the interrotor) is employed. As these constitute the stator for the internal induction machine, n_T acts as its synchronous speed. The EVT inner rotor also has a three pole pairs winding.

4) A centrifugal pump that takes from the EVT output shaft a maximum mechanical power of P_{Pmax}=75kW, at n_{Pmax}=1500RPM, was chosen.

The pump power is greater that the turbine power because is made up of two components: the power P_{rei} transmitted electromagnetically from the interrotr to the inner rotor P_{rei} and the power P_{irVFD} supplied for the irVFD, i.e., $P_P=P_{rei}+P_{irVFD}$, see Figure 4.

Figure 5 shows the locus of the operating points of the turbine and the centrifugal pump. Since the turbine drives the EVT's interrotor as a weak grid-tie induction generator, the rotational speed will be very close to the synchronous speed n_S defined by the grid frequency. On the other hand, as the selected speed of the turbine has been matched close to n_S, it will always supply maximum power to the interrotor shaft. Thus, the operating point of the turbine is closely defined, except for the slip, by (n_T, T_T) (point A, Figure 5), shown together with the hyperbola (in red) that contains all the points of the T-n plane that has a power value equal to the turbine one of P_T=50kW. Otherwise, the operating points of the centrifugal pump (n_P, T_P) define a parabola (in blue), in accordance with (12). As well as there is a maximum pump speed at n_{Pmax}=1500RPM (point E, Figure 5), a minimum value is considered at n_{Pmin}=500RPM (point B, Figure 5) below which pump operation is not expected. This could be the minimum threshold to overcome the static hydraulic head of the irrigation facility. Also, there is a particular pump speed value n_e in which the mechanical power required by the pump is equal to the power delivered by the turbine (point D, Figure 5). Using the values stated foregoing to compute (12), a n_e=1310 RPM is obtained.

The rectangles depicted in Figure 5, defined by pump and turbine speed with their corresponding torques, reveal the distribution of power flow through the ports of the EVT machine. From the above discussion, it is then clear that the EVT operates with a variable transmission ratio and that a particular power distribution will be given for each pump speed.

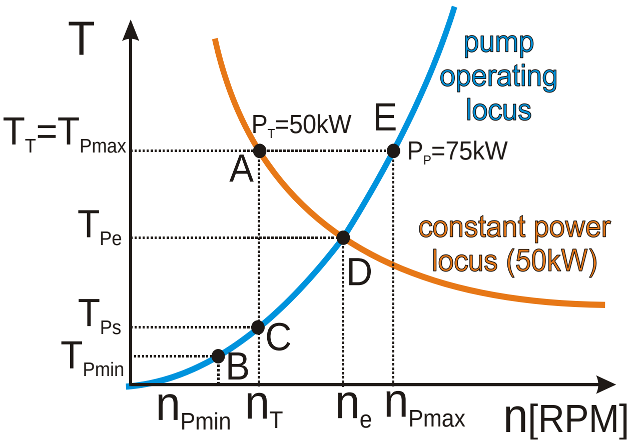

Fig. 5: Operating points locus of the turbine and the centrifugal pump.

Figure 6 shows how the magnitudes previously shown in Figure 5, and the rectangles that represent the associated powers, take on distinctive relative proportions in different working situations. For a better understanding, the representation in the T-n plane is accompanied by a diagram of the EVT showing the power flow direction in its ports for each case. The analysis is carried out at some operating points in the T-n plane that are representative of typical situations, characterized by a particular set of power flow directions. What happens at the points that are at the boundary between two consecutive situations are also discussed. The changing physical variable is the pump speed, which is directly related to the water flow requirement for irrigation, see (16).

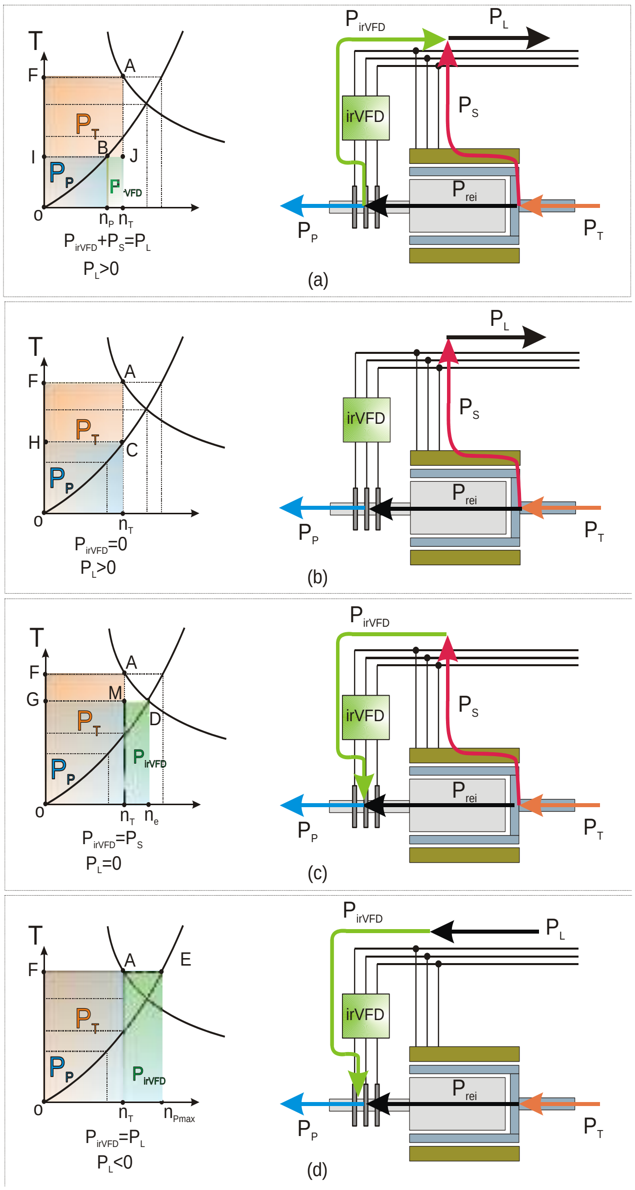

Fig. 6: EVT power flow for different pumps speeds. a) $n_{Pmin}<n_P<n_T$, b) $n_P=n_T$, c) $n_T<n_P<n_e$, d) $n_P=n_{Pmax}>n_T$.

Situation 1 ($n_{Pmin}<n_P<n_T$) (Figure 6 (a) through (b)). In this region, the mechanical power consumed by the pump P_P (rectangle defined by points o-I-B-n_p of Figure 6 (a) through o-H-C-n_T) is lower than the supplied by the hydro-turbine P_T ($P_P<P_T$) (o-F-A-n_T). As the torque demanded by the pump T_P is lower than the produced by the turbine T_T, the stator winding will deliver a power $P_S=P_T-P_{rei}=(T_T-T_P)(2\pi n_S/60)$ into ACN, where P_{rei} is the power transmitted mechanically by the EVT from the interrotor to the inner rotor. On the other hand, the pump speed is lower than n_T and therefore, the inner rotor currents should be in negative sequence. Consequently, the inner rotor is working in generation mode and its power is collected by the irVFD and delivered to the ACN. Both the stator winding power and the irVFD power are injected to ACN and are available to be consumed by residential loads (I-F-A-J-n_T-n_P-B). This power is $P_L=P_S+P_{irVFD}=P_T-P_P$. As a limiting case of this region, when $n_P=n_T$, the inner rotor winding is fed with zero frequency (CC) and P_{irVFD} is approximately zero (Figure 6 (b)).

Situation 2 ($n_T<n_P<n_e$) (Figure 6 (b) through (c)). In this region, the mechanical power taken for the pump (o-H-C-n_T of Figure 6(b) through o-G-D-n_e of Figure 6(c)) is lower than that delivered by the turbine ($P_P<P_T$). The torque demanded by the pump keeps being lower than the turbine's and the stator winding delivers a power $P_S=(T_T-T_P)(2\pi n_S/60)$ to the ACN. On the other hand, the pump speed is higher than n_T and therefore, the irVFD feeds the inner rotor with a positive sequence. Because of this, the inner rotor is working in motoring mode, and the irVFD supplies it with a power that in turn is taken from the ACN. The net remaining electrical power available for residential loads is $P_L=P_S-P_{irVFD}=P_T-P_P>0$. A limiting case of this region is when $n_P = n_e$, in which $P_L=0$ since $P_T=P_P$ and $P_S=P_{irVFD}$. This is clearly noticed from Figure 6 (c), where the rectangles G-F-A-M and n_T-M-D-n_e have equal areas.

Situation 3 ($n_e<n_P<n_{Pmax}$) Figure 6 (c) through (d). In this region, the mechanical power taken for the pump (o-G-D-n_e from Figure 6 (c) through o-F-E-n_{Pmax} of Figure 6 (d)) is greater than that supplied by the hydro-turbine ($P_P>P_T$). The torque demanded by the pump keeps to be lower than turbine's and the stator winding will deliver a power $P_S=(T_T-T_P)(2\pi n_S/60)$ to the ACN. On the other hand, the pump speed is still higher than n_T and therefore the irVFD feeds the inner rotor with a positive sequence. Therefore, the inner rotor is in motoring mode and the power is taken from the ACN through the irVFD. The net power taken from the grid being equal to: $P_L=P_{irVFD}-P_S=P_P-P_T<0$. The limiting case of this region occurs when $n_P=n_{Pmax}$, $P_S=0$ since $T_T=T_P$ and $P_{rei}=P_T$. It also occurs that the irVFD provides the maximum required power $P_{irVFD}=P_{irVFD\_MAX}=$

P_{Pmax}-P_T=25kW to meet the pump's power requirement.

4 Simulation Results

To verify the validity of the theoretical and graphical analysis previously presented in Section 3, a series of simulations were carried out. To perform them, a computer model of the irrigation system has been built, based on the equations presented in Section 2 and implemented using existing blocks in the MATLAB-Simulink package library. This dynamic model allows not only the study of the power distribution in steady state (predicted by the analysis done in Section 3) but is also capable of representing the temporal evolution from one state to another. The numerical values of the most salient parameters of the system model, are given below:

Turbine:

Semi-Kaplan type, rated power P_{TA}=50kW at n_{TA}=1000RPM (see Figure 3), rated efficiency n_T=87%, optimal speed n_{Topt}=900RPM, runaway speed n_{Tmax}=1800RPM, total head (static and dynamic) H=6.5m, rated flow Q=0.922m^3/s.

EVT:

External IM: rated power P_S=50kW (input shaft mechanical power), stator: 3-phase 3 pole- pair winding directly connected to the AC grid, rotor: squirrel cage type, rated slip s=5%.

Internal IM: rated power P_{ir}=75kW (output shaft mechanical power), stator: 3-pole PM array, internal rotor: 3-phase 3 pole-pair winding fed by and ideal irVFD, rated slip s=5%.

Centrifugal pump: maximum mechanical power P_{Pmax}=75kW at n_{Pmax}=1500RPM. The pump speed is adjusted by a PI control loop (with a nested internal torque loop) in the irVFD.

Weak grid:

380VAC/50Hz

To facilitate the comparison between the values obtained by simulation and the ones predicted by theoretical analysis, an ascending pump speed n_P profile with a stepped waveform has been considered. The values of each step are: 500, 1000, 1310 and 1500RPM, which are in correspondence to the points B, C, D and E of Figure 6. The transitions of the speed profile were made smooth, with the intention of representing a typical control action to change the flow for maintaining a desired water level in the irrigation reservoir.

Figure 7 shows how the torque of the different system components evolve over time as the speed of the pump varies, Figure 7 (a). Figure 7 (b) shows the electromagnetic torque of the internal rotor necessary to drive the pump at the desired speed, opposing the antagonistic torque exerted by the pump on its shaft, Figure 7 (c). An excess of electromagnetic torque (with respect to the stationary value) is appreciated, which is associated with overcoming the internal rotor and pump assembly inertia. The torque with which the hydraulic turbine drives the interrotor of the EVT is shown in Figure 7 (d), can be seen that (after the initial start-up transient) it is almost constant, since the speed of the turbine, Figure 7 (f), is always close to its rated value of 1000RPM. This is so because the EVT input shaft speed is practically fixed by the EVT External IM, whose stator presents a resistant electromagnetic torque (Figure 7 (e)), which varies abruptly with small speed changes, due to the high slope of its torque-speed characteristic (denoted as K_G in (10)). Regarding T_{EM1}, it can be seen how it decreases as the torque transmitted to the pump shaft by electromagnetic means, T_{EM2}, increases.

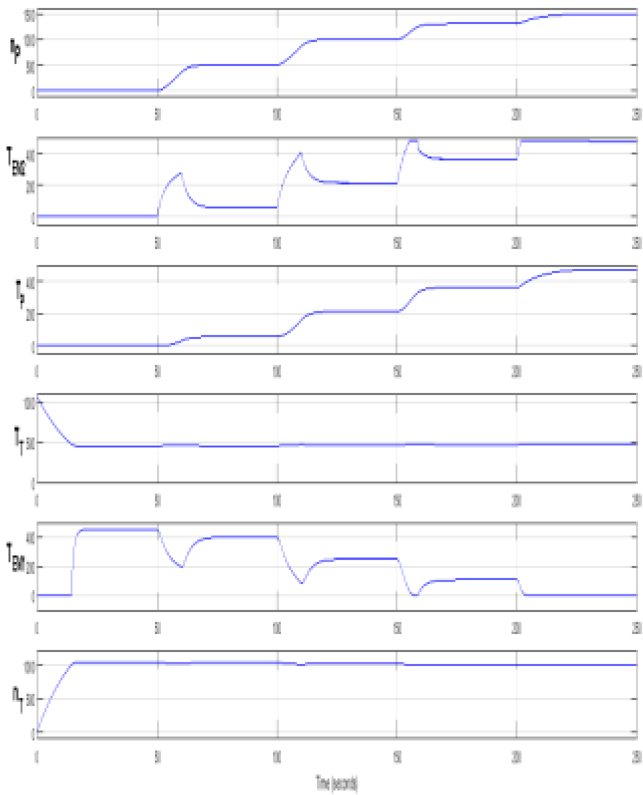

Fig. 5: System torques evolution during pump speed changes.

The rounded value of the system torques and turbine speed for each pump speed are shown in Table 1.

Table 1. System torque values in [Nm] and turbine speed, for each pump speed, in [RPM].

n_P	T_{EM2}=T_P	T_T	T_{EM1}	n_T

0	0	451	451	1043
500	54	454	400	1038
1000	212	463	251	1024
1310	362	471	109	1010
1500	475	475	0	1000

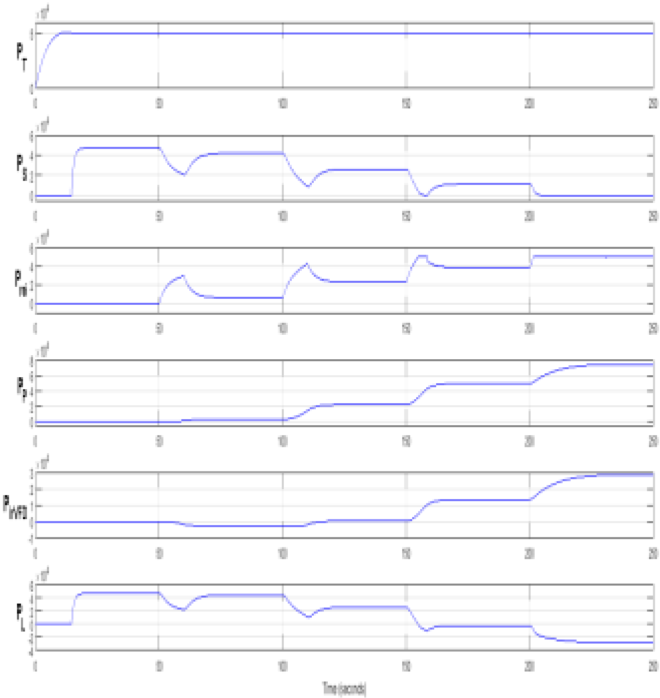

Fig. 8: System powers evolution during pump speed changes.

Table 2. System power values, in [kW], for each pump speed, in [RPM].

n_P	P_T	P_S	P_{rei}	P_P	P_{irVFD}	P_L
0	49.3	47.3	0	0	0	47.3
500	49.4	41.9	5.9	2.9	-2.9	45
1000	49.6	26.3	22.7	22	0.2	26
1310	49.8	11.5	38.3	49.5	13.3	-2
1500	49.9	0	49.9	74.2	28.2	-27

Figure 8 shows the evolution of the powers in the different components of the system, associated with torques and speeds shown in Figure 7. Firstly, Figure 8 (a) shows the mechanical power supplied to the EVT input shaft from the turbine, which remains practically at its rated value of 50 kW, as it was previously explained. The electrical power generated by the stator of the EVT External IM is shown in Figure 8 (b). This power is obtained by subtracting from the turbine power, the mechanical power transmitted via electromagnetic coupling to the internal rotor, shown in Figure 8 (c). Figure 8 (d) shows how the mechanical power demanded by the pump increases as its speed increases. This power is supplied in part by the transmitted power, and partly by the irVFD, shown in Figure 8 (e). Finally, Figure 8 (f) shows the power flowing through the link that connects the irrigation station to the weak grid and the residential loads, which is formed by the power supplied by stator of the EVT External IM minus the power absorbed by the irVFD. The rounded values of different system powers for each pump speed value are listed in Table 2.

The obtained simulation results show a good correlation with the theoretical analysis carried out in Section 3, thus demonstrating its validity.

5 Conclusions

In this work, an irrigation system for rural areas has been proposed. It is suitable for the case where, in addition to disposing of the essential water resource, there is a weak distribution grid with a power capacity enough to supply existing residential loads, but it is incapable to deliver the power required for irrigation purposes. As it was conceived, the system presents some novel aspects and very interesting advantages:

- The centrifugal pump, responsible for feeding water to the elevated reservoir, is coupled to a Semi-Kaplan microturbine through an EVT Induction Machine (IM). This provides higher efficiency than the traditional system, based on two electrical machines interconnected by variable frequency drives that must handle the system full power.
- The proposed EVT is based exclusively on induction machines, both for the External and Internal Machines. This makes the coupling very simple, reliable, and robust.
- The EVT External IM stator winding is directly connected to the AC grid, avoiding the use of an expensive and complex electronic converter. Any synchronization mechanism with the grid is not needed. Simple soft-start equipment is only required.
- The EVT Internal IM rotor winding is powered by a VFD for adequate control and variation of the centrifugal pump speed. This means that the VFD only must handle a fraction of the total pumping power.
- The micro-hydro turbine operates at almost fixed speed, delivering its rated power all the time. Thus, the best use of its capacity is achieved.
- An adequate component sizing makes it possible to achieve a limited power exchange with the weak grid. When the pump power exceeds the power delivered by the turbine (50kW), some assistance from the weak grid is required. The power taken from the grid reached the moderate amount of

25kW, in the worst case (maximum pumping power).

Regarding the operation of the proposed system, an analytical and graphic study has been carried out to evaluate the distribution of mechanical and electrical powers among its components, including the exchange with the weak grid, for typical working situations defined by different pump speeds. The results obtained through computer simulations have shown very good agreement with the analytical results and there were no anomalies in the transition between stationary operating points.

As a future work, it is planned to explore the possibility of including a high-capacity storage system for maximum usage of the hydraulic resource and minimum power exchange with the weak grid. The flow battery is a very attractive device for this application. To reach the proposed objectives, a relatively complex supervisory control system must be developed, to manage and coordinate the energy interchange between the system components. Both topics will be the subject of future research.

Acknowledgement:
The authors express their gratitude to UNLP, CONICET, CIC, and ANPCyT, since without the support of these institutions, this work would not have been possible.

References:
[1] López-González, A., Ferrer-Martí L., Domenech B., “Long-term Sustainability Assessment of Micro-hydro Projects: Case Studies from Venezuela”, *Energy Policy*, Vol. 131, 2019, pp. 120–130.
[2] Fontela, C. et al., “Riego por Goteo en Mendoza, Argentina: Evaluación de la Uniformidad del Riego y del Incremento de Salinidad, Sodicidad e Iones Cloruro en el Suelo”, *Revista de la Facultad de Ciencias Agrarias-Universidad Nacional de Cuyo (UNC)*, Vol. XLI, No. 1, 2009, pp. 135-154.
[3] Shaikh Abdullah Al Mamun Hossain et al. “Contemporary Perspective of Drip Irrigation”, *Asian Research Journal of Agriculture*, Vol. 3, No. 4, 2017, pp. 1-22.
[4] Reyna, M.T. et al. “Turbinas Hidroeléctricas Michell Banki para Aplicación en Comunidades”, *Avances en Energías Renovables y Medio Ambiente (AVERMA)*, Vol. 15, 2011, pp. 59-66.
[5] Bhatnagar, P. and Srivastava, R., “Gravity-fed Drip Irrigation System for Hilly Terraces of the Northwest Himalayas”, *Irrigation Science*, Vol. 21, 2003, pp. 151–157.
[6] Villar. E., Puertas, C. and Barcia F., “Procesos de Innovación Tecnológica y Organizacional Asociados al Uso del Recurso Hídrico del Área de Riego de La Hijuela 22 del Canal Sud Alto Verde en San Martin, Mendoza”, *VI Jornadas de Actualización en Riego y Fertirriego*, Mendoza, nov. 7, 8 y 9, 2012, pp. 1-9.
[7] A. Wibisono, L. H. Pratomo and A. K. D. Santoso, "Feasibility Study Analysis on Run-Off-Natural River Mini-Hydro Power Plant Business Development," *2021 International Conference on Technology and Policy in Energy and Electric Power (ICT-PEP)*, Jakarta, Indonesia, 2021, pp. 318-323.
[8] Syahputra, R. and Soesanti, I., “Planning of Hybrid Micro-Hydro and Solar Photovoltaic Systems for Rural Areas of Central Java, Indonesia”, *Journal of Electrical and Computer Engineering*, Vol. 2020, pp. 1-16, 2020.
[9] Indiveri, N. et al., “Estudio Exploratorio para el Aprovechamiento de Pequeñas y Medianas Centrales Hidroeléctricas en Áreas de Estudio Pertenecientes al Oasis Norte de la Provincia de Mendoza”, 2010, *Edited by (UNC)*, pp. 1-73.
[10] Patel, H and Sunetra Chowdhury, “Cost Effective Microhydro-based Microgrid Schemes for Rural Electrification in South Africa”, *53rd Int. Universities Power Engineering Conf. (UPEC)*, Glasgow, UK, 04-07 September, pp. 1-6, 2018.
[11] Angadi, S. et al., "Comprehensive Review on Solar, Wind and Hybrid Wind-PV water Pumping Systems- An Electrical Engineering Perspective," *IEEE Transactions on Power Electronics and Applications*, Vol. 6, no. 1, pp. 1-19, 2021.
[12] “Variable Speed Drive (VSD) for Irrigation Pumping Tech Note”, *USA Dept. of Natural Resources Conservation Service* https://directives.sc.egov.usda.gov/OpenNonWebContent.aspx?content=32786.wba
[13] Hoeijmakers, M.J. and Ferreira J.A., ‘‘The Electric Variable Transmission’’, *IEEE Trans. Ind. Appl.*, Vol. 42, no. 4, 2006, pp. 1092–1100.
[14] J. Druant, H. Vansompel, F. De Belie and P. Sergeant, "Efficiency of a CVT-Operated EVT Experimentally Evaluated Against Half-Toroidal and Push-Belt CVTs," in *IEEE Transactions on Industrial Electronics*, vol. 65, no. 4, pp. 3095-3103, April 2018, doi: 10.1109/TIE.2017.2756589.

[15] Q. Xu et al., "Research on the Efficiency Optimization Control of the Regenerative Braking System of Hybrid Electrical Vehicle Based on Electrical Variable Transmission", *IEEE Access*, vol. 7, 2019, pp. 116823-116834.

[16] Y. Zhu and C. Cai, "Current Source Converter Based Control Strategies for the DPF-WECS," *21st International Conference on Electrical Machines and Systems (ICEMS)*, Jeju, Korea (South), 2018, pp. 1105-1109.

[17] M. Kral, R. Gono and M. Gono, "Implementation of Small Hydro Power Plants in Water Facilities," *2019 20th International Scientific Conference on Electric Power Engineering (EPE)*, Kouty nad Desnou, Czech Republic, pp. 1-4, 2019.

[18] Azimov, U. and Avezova, N., "Sustainable Small-scale Hydropower Solutions in Central Asian Countries for Local and Cross-border Energy/water Supply", *Renewable and Sustainable Energy Reviews*, Vol. 167, 2022, pp. 1-14.

[19] Okot, D.K., "Review of Small Hydropower Technology", *Ren. and Sust. Energy Reviews*, Vol. 26, 2013, pp. 515–520.

[20] Quaranta, E., "Optimal Rotational Speed of Kaplan and Francis Turbines with Focus on Low-Head Hydropower Applications and Dataset Collection", Journal of Hydraulic Engineering. Vol. 145, No. 12, 2019, pp. 4019043-1/4019043-5.

[21] Abeykoon C., "Modelling and Optimisation of a Kaplan Turbine - A Comprehensive Theoretical and CFD Study", *Cleaner Energy Systems*, Vol. 3, 2022, pp. 1-31.

[22] Ansel, A., Robyns, B., "Modelling and Simulation of an Autonomous Variable Speed Micro Hydropower Station", *Mathematics and Computers in Simulation*, Vol. 71, Issues 4–6, 2006, pp. 320-332.

[23] Druant, J. et al., "Field-Oriented Control for an Induction-Machine-Based Electrical Variable Transmission", *IEEE Transactions on Vehicular Technology*, Vol. 65, no. 6, 2016, pp. 4230-4240.

[24] B. K. Bose, *Modern Electronics and AC Drives 1st Edition*, Pearson Education, India, 2015.

[25] Mokeddem, A. et al., "Performance of a Directly-coupled PV Water Pumping System", *Energy Conversion and Management*, Vol. 52, No. 10, 2011, pp. 3089-3095.

[26] Esmaeilian, H. et al., "Design Methodology to Optimise Induction Machines Based Stand-alone Electrical Wind Water Pumping Systems", *IET Electr. Power Appl.*, Vol. 13, No. 12, pp. 2058-2069, 2019.

Contribution of Individual Authors to the Creation of a Scientific Article (Ghostwriting Policy)

Marcelo G. Cendoya has conducted the research on the semi-Kaplan turbine, focusing on its design parameters and sizing for the studied application. He has developed the system model and has carried out the computer simulation. He has participated in the conception of the system topology. He has collaborated with the writing and revision of the manuscript.

Santiago Verne has conducted the research on irrigation systems and on EVT devices. He has participated in the conception of the system topology. He has collaborated in the system analysis. He did the writing of the manuscript and its editing. He has made the figures.

Pedro E. Battaiotto has collaborated in the conception of the system topology and the analysis of the EVT operation inside the system. He has carried out the revision and correction of the manuscript.

Sources of Funding for Research Presented in a Scientific Article or Scientific Article Itself

UNLP Proyecto 11/I255 *"Electrónica de Potencia y Sistemas de Control Avanzado Aplicados a Fuentes de Energía Alternativas"*. 1/2020 - 12/2023.

CONICET PIP 112-2020-0102801CO *"Control Avanzado y Electrónica de Potencia Aplicados a la Optimización de Sistemas Basados en Energías No Convencionales"*. 12/2021 – 12/2024.

ANPCyT PICT N°2018-03747 *"Control, Electrónica e Instrumentación: Aplicaciones en Energías Alternativas e Ingeniería Biomédica"*. 11/2019 – 11/2022.

Conflict of Interest

The authors have no conflicts of interest to declare that are relevant to the content of this article.